EMPIRICAL ORTHOGONAL FUNCTION ANALYSIS OF SATELLITE-DERIVED CURRENTS IN THE TROPICAL ATLANTIC

Isabelle VILELA[1]*; Moacyr ARAUJO[1,2]; Pedro TYAQUIÇÃ[1]; Dóris VELEDA[1]

[1]Department of Oceanography, Federal University of Pernambuco, Recife, PE, Brazil. E-mail: isabelle.vilelaoliveira@ufpe.br, moa.ufpe@gmail.com, tyaquica@gmail.com, doris.veleda@ufpe.br
*Corresponding author

[2]Brazilian Research Network on Global Climate Change, São Paulo, SP, Brazil.

RESUMO. Uma análise da Função Ortogonal Empírica foi realizada usando 22 anos de correntes superficiais mensais para investigar os principais modos de variabilidade da circulação superficial do Atlântico Tropical (AT) com base em dados de satélite. O primeiro modo da componente zonal retém mais de 50% e o segundo 8% da variância total, representando respectivamente o ramo central da Corrente Sul Equatorial (cCSE) e um dipolo zonal com um sinal positivo para o oeste, e um negativo para leste na região da Língua Fria do AT. O primeiro modo meridional explica 18% da variância total, com alternância de estruturas positivas e negativas no norte do AT Ocidental, representando a alta dinâmica associada à retroflexão da Corrente Norte do Brasil (CNB) e seus vórtices anticiclônicos. O segundo modo meridional (cerca de 12%) representa a alta variabilidade da CNB. No primeiro modo da velocidade das correntes predomina o padrão da cCSE (30%) e o segundo (8%) representa o dipolo zonal entre a piscina quente do AT e a Língua Fria do Atlântico. Estes modos dominantes de variabilidade das correntes superficiais contribuem para a compreensão dos processos de interação oceano-atmosfera, variabilidade do transporte meridional e zonal, e a dinâmica da superfície no AT.

Palavras-Chave: Função Ortogonal Empírica, Sensoriamento Remoto, Correntes Oceânicas, Dinâmica dos Oceanos, Atlântico Tropical.

ABSTRACT. An Empirical Orthogonal Function (EOF) analysis was performed using 22 years of monthly surface currents in order to investigate the main modes of variability of the Tropical Atlantic surface circulation based on satellite data. The EOF1 of the zonal component captures more than 50% of the total variance and represents the central branch of the South Equatorial Current (cSEC). The EOF2 of the zonal component (~8% variance) represents a zonal dipole with a positive signal to the west, and a negative one to the east in the Atlantic Cold Tongue (ACT). The meridional EOF1 (18% variance), with alternating positive and negative structures in the western tropical North Atlantic, representing the high dynamics associated to the North Brazil Current retroflection and its anticyclonic eddies. The meridional EOF2 (~ 12% variance) represents the high variability of the NBC, with stronger intermittent signals propagating from the eastern Atlantic. In the EOF1 of currents speed predominates the cSEC pattern (30%) and the EOF2 (8%) represents the zonal dipole between South Atlantic Warm Pool and the ACT. These dominant modes of surface current variability contribute to the understanding of the ocean-atmosphere interaction processes, zonal and meridional transport variability, and the surface dynamics in the TA.

Keywords: EOF Analysis, Remote Sensing, Ocean Currents, Oceanic Dynamics, Tropical Atlantic.

Tropical Oceanography, Recife, v. 46, n. 2, p. 1-24, 2018.

1

INTRODUCTION

The pathways and mechanisms of ocean transport are crucial issues in understanding the present state of climate and the possibilities of future changes (Ganachaud and Wunsch, 2000). The surface currents in Tropical Atlantic (TA) are marked by a wide range of space-time variability. In the equatorial ocean region, for example, the variability occurs over a wide range of time and space scales, with a complex area of predominantly zonal currents, composed by westward currents and eastward countercurrents (Arnault and Kestenare, 2004). The upper zonal current system in the tropical Atlantic is of great importance for both interhemispheric and west-to-east exchange of heat, salt, and nutrients (Brandt *et al.*, 2008; Foltz *et al.*, 2003; Kirchner *et al.*, 2009). The TA region is characterized by the presence of two broad, westward flowing currents, the South Equatorial Current (SEC) and North Equatorial Current (NEC). The SEC extends from the surface to 100m depth and it is divided into three branches: the southern South Equatorial Current (sSEC), the central South Equatorial Current (cSEC), and the northern South Equatorial Current (nSEC). Near the Brazilian coast, the sSEC bifurcates giving origin to western boundary currents: Brazil Current (BC) and North Brazil Undercurrent (NBUC). The sSEC bifurcation has a climatological mean position in about 15° S, with a southernmost position in July, and a northernmost in November (Rodrigues *et al.*, 2007; Stramma and England 1999).

The southward limb of the sSEC becomes the BC and merges into the South Atlantic subtropical gyre system. The northward limb of the sSEC flows into the NBUC (Stramma and Schott, 1999; Stramma *et al.*, 2005; Veleda *et al.*, 2012) and, as a western boundary current, it carries warm waters from South Atlantic across the equator to the northern hemisphere. The cSEC joins the NBUC near Cape São Roque at 5°S, inducing its vertical structure to change from an undercurrent to a surface-intensified current, resulting in the North Brazil Current (NBC). The NBUC/NBC system supply northward warm-water, as part of the thermohaline overturning circulation (Gordon, 1986; Schmitz, 1995). The NBUC has a mean northward transport along the northern coastline of Brazil, with a seasonal cycle of northward flow maximum in July (Schott *et al.*, 2005).

The NBC flows to the northwest with maximum speeds around 1.0 ms-1 (Richardson *et al.*, 1994), with maximum transport (36 Sv) in July – August, and minimum (13 Sv) in April - May (Johns *et al.*, 1998). This current carries nutrients from the Amazon River discharge northwestward along the Brazilian Shelf (Muller-Karger *et al.*, 2005). The NBC transport is maximum when the current reaches maximum latitude and a ring is shed (Garzoli, 2004). The NBC dynamics produces several mesoscale rings. According to Jochum and Malanotte-Rizzoli (2003), circulation models had showed that NBC retroflection generates around 6 to 7 anticyclonic vortices per year. Theses vortices propagate northwestward along the Guyana coast (Didden and Schott, 1993; Wilson *et al.*, 2002) by the potential vorticity conservation. The

Tropical Oceanography, Recife, v. 46, n. 2, p. 1-24, 2018.

2

detachment of anticyclonic eddies from the NBC retroflection is observed during November through January, when the NBC retroflection into the NECC weakens and finally breaks down (Didden *et al.*, 1993). Moreover, the NBC rings are responsible for more than half of the inter-hemispheric exchange of mass and heat associated with Meridional Overturning Circulation (MOC) (Garzoli *et al.*, 2003). So that, monitoring of the NBC rings on the ocean surface currents variability is important for the climate studies and ocean-atmosphere interaction processes.

The NBC variability is also affected by the direction of the winds in the northern Brazil. Trade winds vary seasonally along with the Intertropical Convergence Zone (ITCZ), which migrates latitudinally from March to April in around 5°S, and in August to approximately 15°N. This ITCZ drives the variability of the trade winds, mainly in the equatorial band, which are predominantly from the southeast during the June to November and from the northeast in December to May in the Tropical Atlantic (Geyer *et al.*, 1996). When the Northeast trade winds are predominant, the NBC is confined along the coast and flows northwestward. However, during the predominant period of the Southeast trade winds, the NBC expands and retroflects eastward between 5° N and 10° N (Bourlès *et al.*, 1999). Consequently, the NBC retroflection feeds the North Equatorial Countercurrent (NECC), with eastward-transported waters, rich in nutrients, from the Amazon River plume (Coles *et al.*, 2013; Fonseca *et al.*, 2004; Richardson and Reverdin, 1987). The NECC has low annual mean velocities of 5-10 cm/s (Richardson and Walsh, 1986), zonal current flows from west to east that varies seasonally.

The NECC flows eastward feeding the Guinea Current (GC) in the eastern TA, which is strongest in the boreal summer (Longhurst, 1962). The GC flows eastward throughout the year, with a maximum mean velocity of 42 cms-1 at 4°N, 7.5°W (Richardson and Walsh, 1986). At south of GC, the Angola Current (AC) is a narrow current and moving fast along the Angola coast in which transports saline and warm water to near the coast (Hardman-Mountford *et al.*, 2003), and it is influenced by Equatorial Atlantic variability (Chang *et al.*, 2008). Another feature near the AC is the Angola Dome (AD), which is a cold region, associated with the cyclonic turn of the South Equatorial Undercurrent (SEUC) (Peterson and Stramma, 1991). The AD forms a cyclonic gyre, centered at 10°S and 9°E, which links the South Equatorial Countercurrent (SECC) with the AC (Doi *et al.*, 2007). North of the Gulf of Guinea, Bakun (1978) found a correlation between intensification of the Guinea Current (GC) and local cooling, since the GC carries cool water from the African coast to center of the basin.

The dominant seasonal SST, with low temperature in the eastern equatorial Atlantic, characterizes the formation of the Atlantic Cold Tongue (ACT) (Caniaux *et al*., 2011). In May–June, the ACT develops rapidly when the ITCZ shifts northward over the eastern Atlantic, with cross-equatorial southerlies intensifying, and reaches its peak in July–August (Okumura and Xie, 2004). The ACT is reduced through weakening of the southerly cross–equatorial winds from September onward (Deppenmeier *et al*., 2016). The covariability of the trade winds over the

western part of the basin with SST and heat content in the eastern TA was analysed by De Almeida and Nobre (2012). These mechanisms compose the Bjerknes feedback (BF), which is responsible for the ACT mode. The ACT has a positive feedback phase peaking during boreal summer, when the Bjerknes feedback is stronger. The Bjerknes feedback consists of three components, which the first one is the influence of SST anomalies in the eastern part of the equatorial Atlantic basin on zonal winds. The second is the effect of the zonal winds anomalies in the western equatorial Atlantic on the Heat Content (HC) of the eastern equatorial Atlantic, and the third one the local effect of the HC anomalies on overlying SSTs in the cold tongue region (Deppenmeier *et al.*, 2016).

The west and east of the TA are not independent of each other; they are related in a high dynamic system. Strength and position of the South Atlantic anticyclone impacts on timing of the ACT (Caniaux *et al.*, 2011), consequently it influences the SST variability over the TA. Moreover, the oceanic pathway consists of westward propagating of the TIWs along the equatorial Atlantic, forced by equatorial zonal wind stress anomalies (Hormann and Brandt, 2009; Servain *et al.,* 1982). Thus, the TA is a region of high interhemispheric heat exchanges, so the study of the surface current dynamics contributes to the understanding of the zonal and meridional transport variability, such as the ocean-atmosphere interaction processes.

The exchanges between ocean and atmosphere in the TA are closely related to processes of global climate change and air-sea CO_2 exchanges distribution, since that the surface currents are the major carriers of heat and nutrients. Thus, the knowledge of the ocean dynamics is necessary for understanding the effects that control the interannual climatic variability and interactions between tropics and subtropics (Schouten *et al.*, 2005). Therefore, the main goal of this study is to estimate the dominant modes of surface current variability in the TA, based on satellite data.

METHODS

The study area comprised the region in Tropical Atlantic from 15° S to 15° N in latitude, and from 70° W to 20° E in longitude (Fig. 1). We used 22 years of monthly horizontal velocity (zonal and meridional components) of surface currents, from 1993 to 2014, with 1/3° grid resolution. The Ocean Surface Current Analyses Real-time (OSCAR) project is a NASA Earth Science funded research project to use satellite fields to create global surface currents (www.esr.org/oscar_index.html) (Dohan and Maximenko, 2010). The OSCAR project attempts to better understand air-sea momentum exchange using satellite observations with simplified physics to calculate global ocean currents (Dohan, 2017). OSCAR currents combine Ekman and geostrophic currents based on QuikSCAT winds and TOPEX Poseidon sea level height measurements (Bonjean and Lagerloef, 2002).

Tropical Oceanography, Recife, v. 46, n. 2, p. 1-24, 2018.

4

Sudre and Morrow (2008) have confirmed, by statistical comparison of the OSCAR products with equatorial current meter velocities, good correlation for both the zonal and meridional velocity components. They also find that the OSCAR product shows higher zonal and meridional correlations along the equator compared to the Centre de Topographie des Océans et de l'Hydrosphère (CTOH) currents. A recent study by Johnson *et al.* (2007) carefully characterized the spatial and temporal resolution of their surface current product, in comparison with the available in situ data (surface drifters, TAO current meter arrays, etc.). They found that in the OSCAR products, the zonal current variability is reasonably accurate in the near-equatorial region, at periods of 40 days and better estimated than the meridional currents. According Sudre and Morrow (2008), CTOH and OSCAR satellite surface products show a high correlation with the zonal surface drifter velocities, particularly around the North Equatorial Current at 10°N, with lower correlations in the southern tropical band. They also find that neither OSCAR and CTOH products captures the meridional current system in the 10° N–10° S band, because these meridional velocities are dominated by tropical instability waves and shipboard ADCP instruments.

In order to estimate the main patterns of surface currents in the TA, Empirical Orthogonal Function analysis (EOF) and their respective Principal Components (PCs) were performed. The EOF can separate the spatial and temporal patterns of the data (Oh and Suh, 2018) and was constructed by a Singular Value Decomposition (SVD) analysis (Bretherton *et al.*, 1992). The scores of the SVD modes were calculated by the squared covariance fraction (SCF) which expresses the percentage of variance explained by the modes. The PCs periodicity were analysed by applying wavelet analysis. The EOF was applied to monthly anomalies of currents. The anomalies were calculated removing the monthly climatology for the 22 years.
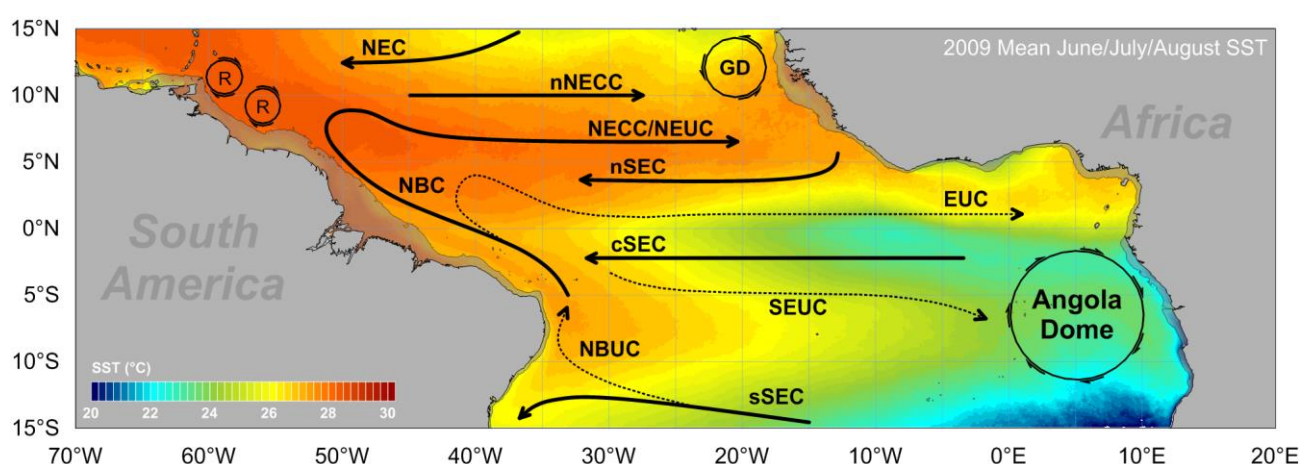

Figure 1. Schematic of surface and subsurface tropical Atlantic Ocean currents. North Equatorial Current (NEC), North Equatorial Countercurrent and Undercurrent (NECC, NEUC), South Equatorial Current with northern, central and southern branches (nSEC, cSEC, sSEC), South Equatorial Undercurrent SEUC), Equatorial Undercurrent (EUC), North Brazil Current (NBC), North Brazil Undercurrent (NBUC), GD (Guinea

Domes), Angola Domes, and the NBC anticyclonic ring (R) displacement. Colored map represents the average SST (June, July and August 2009).

RESULTS

In this section are presented the main modes of variability, identified through the EOF analysis. The EOF mode and its respective Principal Components (PCs) were performed to the surface current velocities as to the zonal and meridional components. The analysed results allowed quantifying the main modes of surface currents in the tropical Atlantic (TA). Associated to each PC we perform the wavelet analysis to detect the main patterns of variability.

EOF ANALYSIS OF THE MERIDIONAL COMPONENTS

The Figures 2-4 represent the main patterns identified in the meridional component. In the first EOF (EOF1), the meridional component explained 18.77% of the total variance (Fig. 2).
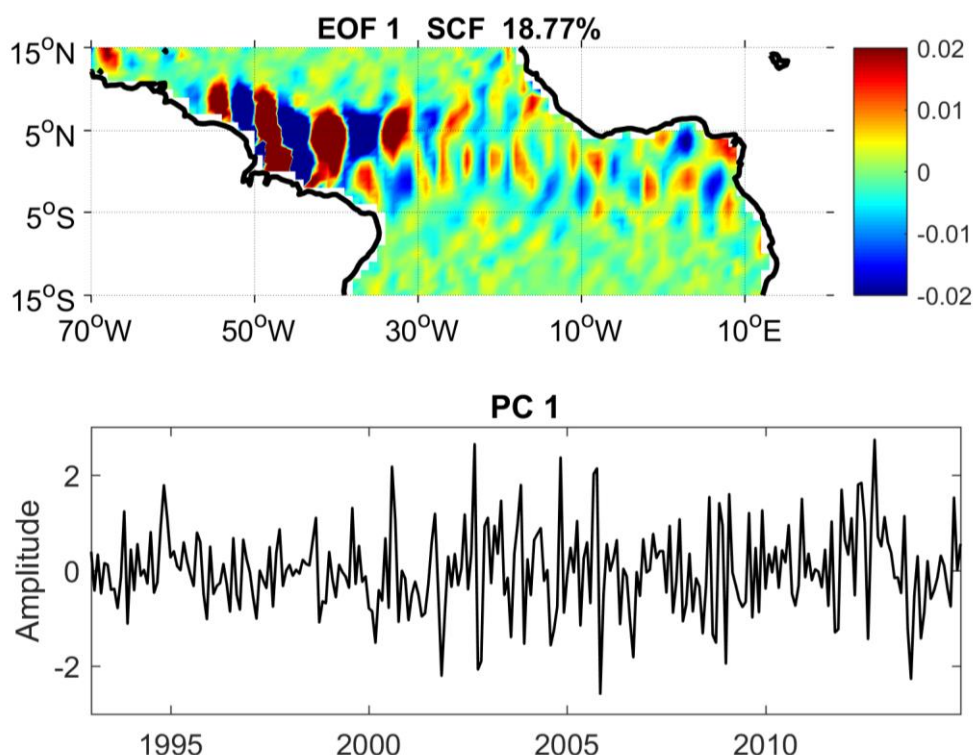

Figure 2. First EOF mode of 22 years of the surface meridional component, the Squared Covariance Fraction (SCF) in percentage, and the first Principal Component (PC1).

The main characteristic of the first mode shows a spatial pattern with alternating positive and negative cores of meridional component. This pattern is confined to the Western Tropical North Atlantic (WTNA), which is a region characterized by strong variability of the NBC

Tropical Oceanography, Recife, v. 46, n. 2, p. 1-24, 2018.

6

retroflection and rings (Johns *et al.*, 1998). In approximately 50°W, where there is the Amazon River, we identify a negative core (southward movement) at the left of the river mouth and a positive core at the right. These alternating cores reach approximately 55°W, which is a predominant limit identified as the NBC retroflection (Fratantoni and Glickson, 2002; Johns *et al.*, 1990). In the eastern Tropical Atlantic, this pattern weakens, and it is not well defined as in the western basin.

The spatial pattern of EOF2 of the meridional component (Fig. 3) corresponded to 11.98% of the covariance. As in the first EOF, the main characteristic of the second mode shows a spatial pattern of alternating positive and negative cores, also confined to the WTNA. We identify a positive core (northward movement) at the river mouth position, followed by negative core displaced to the west. The last positive core more west can indicate the NBC retroflection, in this case positioned approximately at 60W. Comparing the last positive core at west in the WTNA, in the EOF2, with the respective position in EOF1, we identify a westward shift of these alternating signals. The eastern part of the basin shows similar pattern, but weaker in comparison with the WTNA. Nevertheless, the EOF2 exhibits stronger variance in the eastern basin than in the EOF1. The spatial pattern of the second mode in the east side of the basin is well defined, with alternating positive and negative signals, confined between 5° S and 5° N.
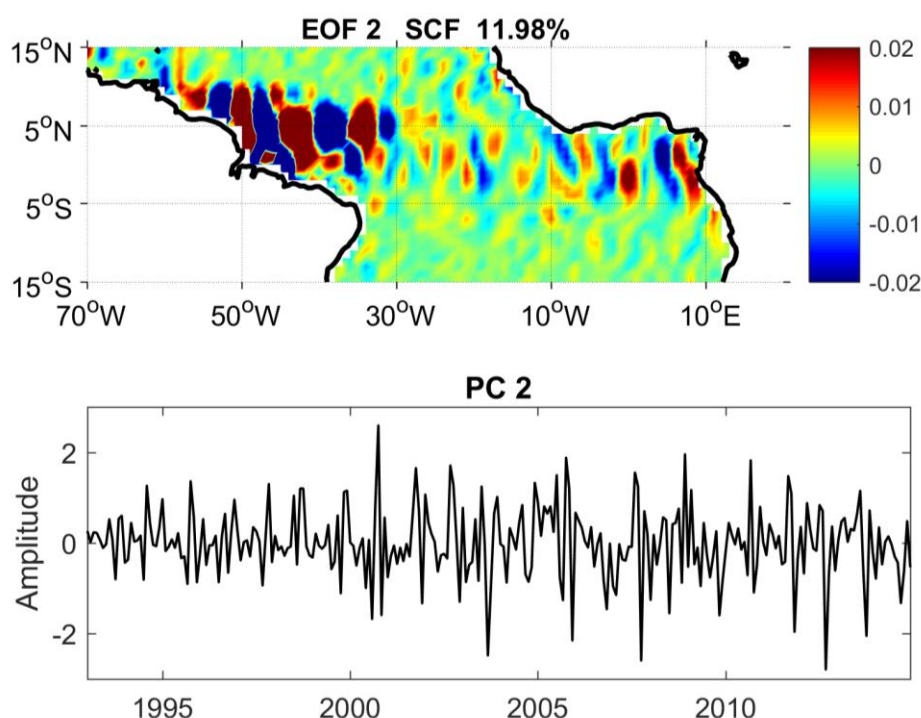

Figure 3. Second EOF mode of 22 years of the surface meridional component, the Squared Covariance Fraction (SCF) in percentage, and the second Principal Component (PC2).

Tropical Oceanography, Recife, v. 46, n. 2, p. 1-24, 2018.

7

The third mode (EOF3) explained 10.29% (Fig. 4) of the total variance. Similar to the first modes 1 and 2, the main spatial pattern of the third mode also shows alternating positive and negative cores in the WTNA. We identify a negative core (southward movement) at the right of the river mouth position, followed by positive core in the west. In this case, high variance exists to the west, with continuous alternating positive and negative signals. The eastern part of the basin shows alternate pattern, but not well defined as in comparison with EOF2.

The EOF4 of the meridional component corresponded 8.97% (not showed), EOF5 retains 5.57% of the total variance (not showed) and showed similar pattern to the EOF1. In these modes, we identify the low variance with continuous alternating cores of positive and negative values, along the equatorial region. However, these structures are better defined in the three first modes. The Principal Components (PCs) are associated with each mode, they showed very similar pattern with high frequency oscillations.
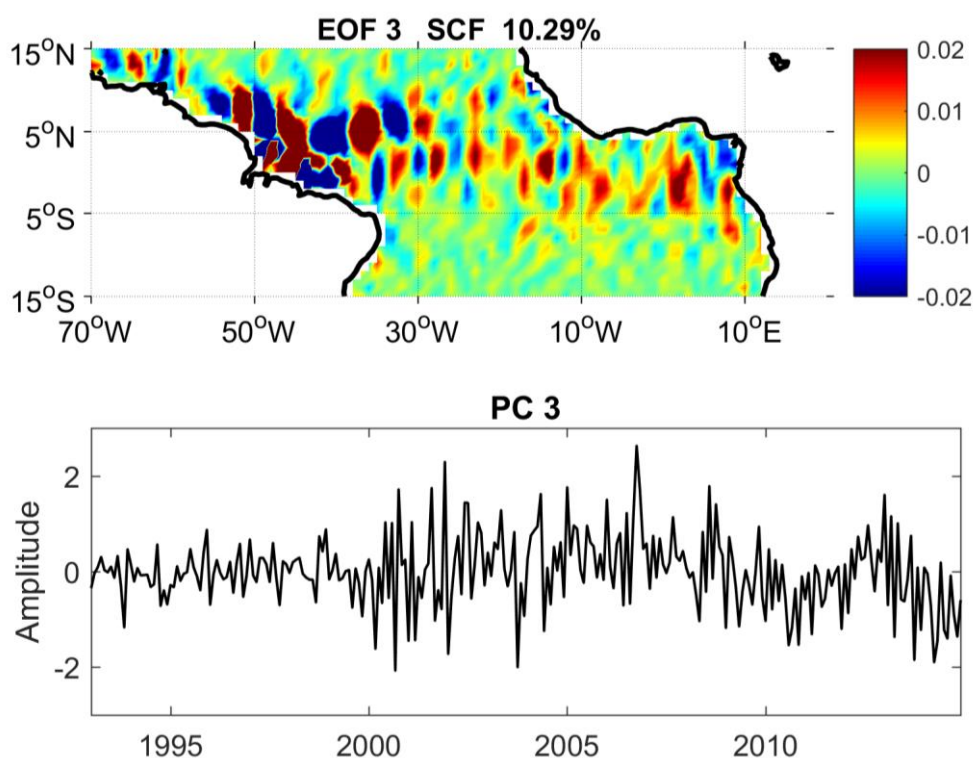

Figure 4. Third EOF mode of 22 years of the surface meridional component, the Squared Covariance Fraction (SCF) in percentage, and the third Principal Component (PC3).

WAVELET ANALYSIS OF THE MERIDIONAL COMPONENTS

For extracting more information, the wavelet analysis is applied and identifies the dominant periodicities from the PCs for the meridional component. The wavelet analyses of the PCs 1, 2 and 3 (Fig. 5) exhibit the periodic components of variability in the time series. The

wavelet of the PC1 showed a strong peak in the variance in 2000 with periodicity about 12 months and intraseasonal peaks in 2002, 2003, 2005, 2008 and 2012. The PC2 showed intraseasonal peaks between 2002, 2003, 2005, 2007, 2011, 2012. A strong and continuous variance signal with about 36 month-period is identified in the years from 2002 to 2008. In the PC3 the strong intraseasonal variance is identified in 2001/2002 and strong annual anomalous signal between 2003 and 2004 and 2007/2008.
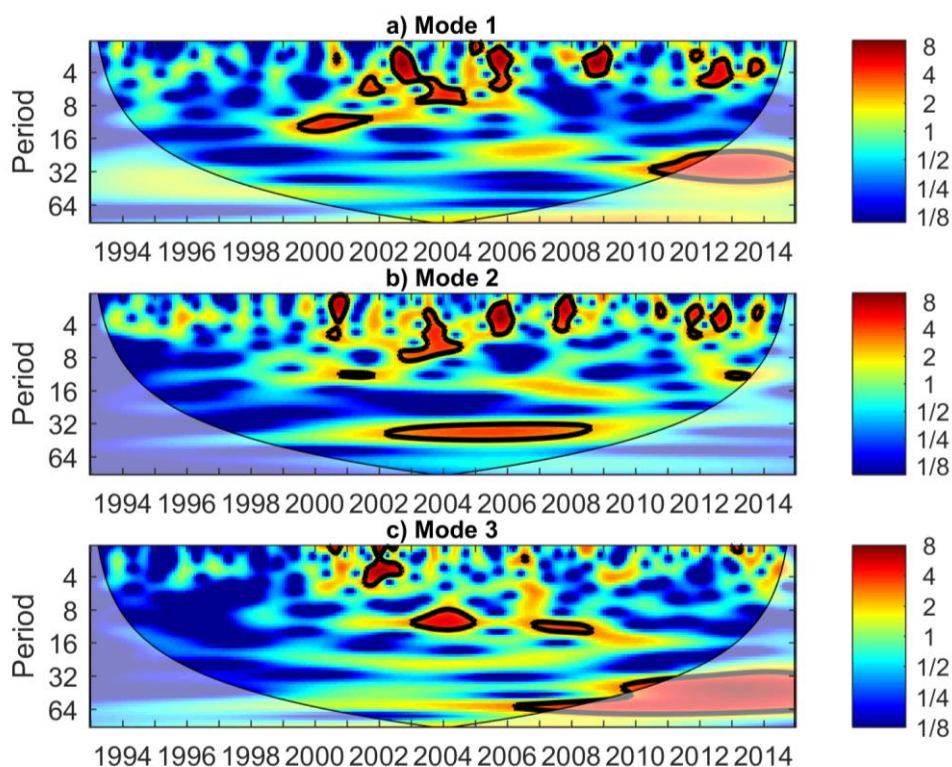

Figure 5. The wavelet transform of the Principal Components (PC1, PC2 and PC3) from the EOF1, EOF2 and EOF3 respectively of the meridional component along the Tropical Atlantic.

EOF ANALYSIS OF THE ZONAL COMPONENTS

The following results (Figs. 6, 7, 8) show the EOF analysis of the zonal components. The first mode (EOF1) corresponded to 50.73% of the total variance (Fig. 6). The spatial pattern shows a negative signal between 5° S - 5° N, which cover the cSEC position (3° - 5° S). This negative signal covers the area from the African coast to the Brazilian coast, and along to the north coast, where it represents the NBC flow. Besides that, at the 7° N, the first mode shows a positive signal flowing eastward, from approximately 51° W to 10° E (Fig. 6), which can be associated to the NECC position.
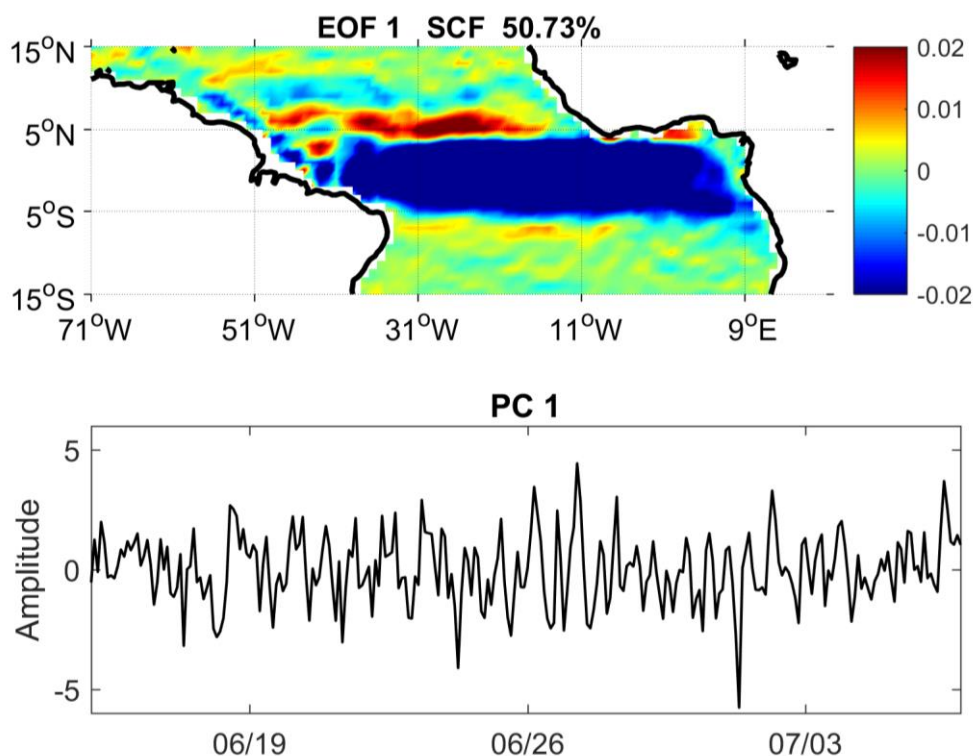
Tropical Oceanography, Recife, v. 46, n. 2, p. 1-24, 2018.

9

Figure 6. First EOF mode of 22 years of the surface zonal component, the Squared Covariance Fraction (SCF) in percentage, and the second Principal Component (PC1).

The second mode (EOF2) of the zonal component explained 8.23% of the total variance (Fig. 7). The EOF2 shows a positive signal in the WTNA. This positive signal exists along the north Brazil coast. North of the positive signal in the WTNA, there is a negative signal approximately 7-8° N, which is associated with the NECC, this negative signal is an interannual pattern. This signal is followed at north by a positive signal. In the eastern equatorial Atlantic, a negative signal exists from the African coast to the middle of the basin at the same area of the cold tongue. This zonal dipole is associated with the Bjerknes feedback (BF), once the BF is stronger when the cold tongue shows a positive phase peaking during boreal summer (De Almeida and Nobre, 2012; Deppenmeier *et al.*, 2016).

The third mode (EOF3) represents 5.67% of the total variance (Fig. 8), with a positive signal around 7°N flowing approximately from the 50°W to 10°W (Fig. 8), related to the NECC position. Approximately between 3° S and 5° N, a predominant negative signal, indicating a westward flow, crossing the Atlantic basin, and then flowing north-westward along the north Brazil coast, as the NBC position. Further South, between 3°-5° S, a positive signal indicates eastward flow, from the Brazilian coast to African coast.
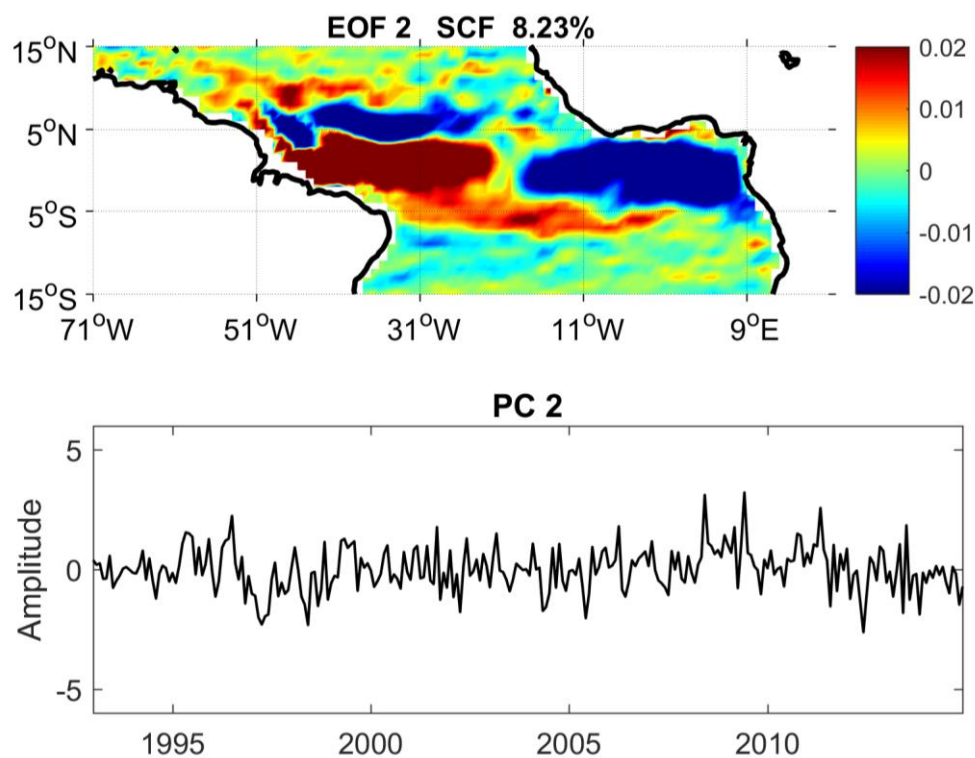
Tropical Oceanography, Recife, v. 46, n. 2, p. 1-24, 2018.

10

Figure 7. Second EOF mode of 22 years of the surface zonal component, the Squared Covariance Fraction (SCF) in percentage, and the second Principal Component (PC2).

Figure 8. Third EOF mode of 22 years of the surface zonal component, the Squared Covariance Fraction (SCF) in percentage, and the second Principal Component (PC3).

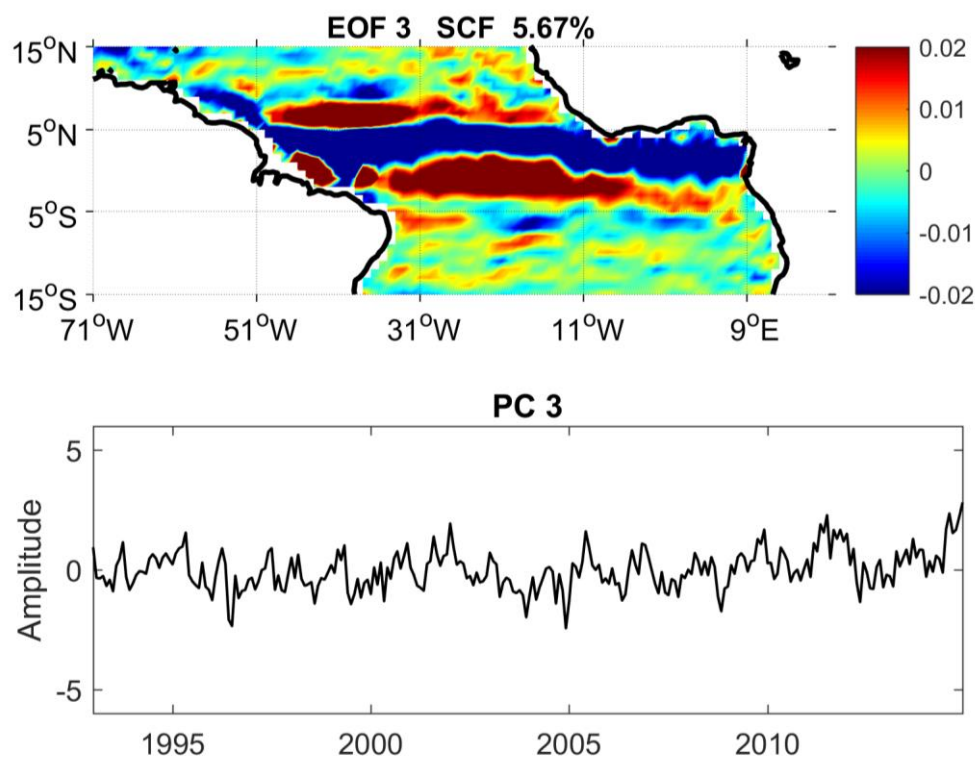**Tropical Oceanography**, Recife, v. 46, n. 2, p. 1-24, 2018.

11

WAVELET ANALYSIS OF THE ZONAL COMPONENTS

For the zonal component, the wavelet analyses of the PC1 presents the strongest variance signal with12-month and 6-month period mainly in 2004-2005 and 2008-2009 (Fig. 9). The years 2004-2005 were marked by the negative phase of Atlantic Niño, which explain strongest southeasterly winds and strong positive zonal currents anomaly. The strong variance identified in 2008 coincides with a strong negative anomaly in the PC1 and a positive phase of Atlantic Niño. In the PC2, the dominant periodicities of strongest variance are in the annual band, between 1997 and 1999, and for 32-month period from the 1996 to 1999 and a strong interannual signal in the years 2008 to 2011. In PC2 also were identified intraseasonal peaks in the variance in 1998, 2001, 2009 and 2012. For the wavelet analyses in the PC3, two intraseasonal peaks were showed in 1996 and 2004, one for 16-month period between 2005 and 2007, and another for 24-month period during 2010 and 2011 (Fig. 9).
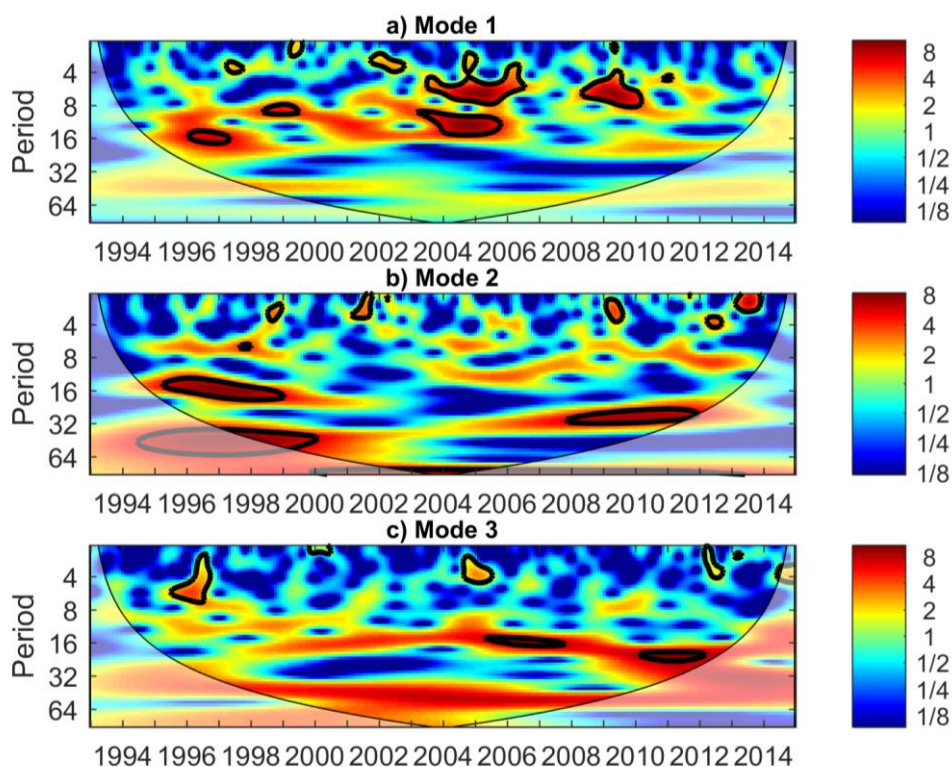

Figure 9. The wavelet transform of the Principal Components (PC1, PC2 and PC3) from the EOF1, EOF2 and EOF3 respectively of the zonal component along the Tropical Atlantic.

EOF ANALYSIS OF THE SURFACE CURRENT VELOCITIES

The next results show the EOF of the current speed (Figs. 10, 11, 12). The variance explained by the first mode (EOF1) of the surface currents retains 30.03% (Fig. 10) of the total

Tropical Oceanography, Recife, v. 46, n. 2, p. 1-24, 2018.

12

covariance. Besides, in the EOF1 there is a dominant negative signal, covering a broad area between5ºS at 5ºN and 50ºW at 5ºE (Fig. 10).
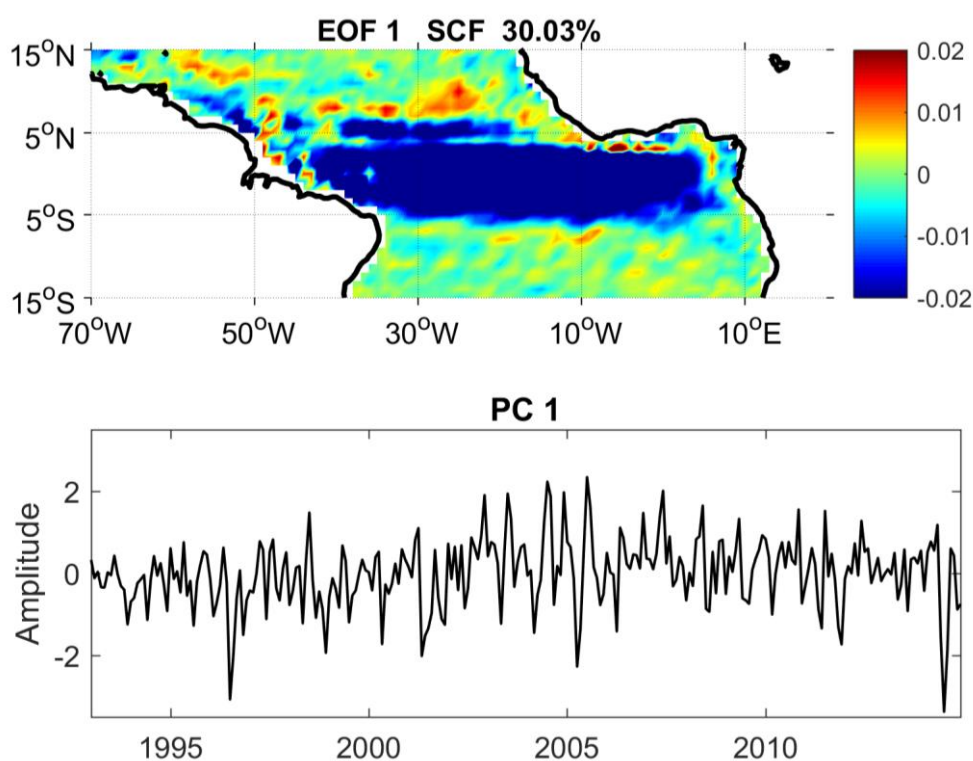

Figure 10. First EOF mode of 22 years of the surface current speed, the Squared Covariance Fraction (SCF) in percentage, and the second Principal Component (PC1).

The second mode (EOF2) retains 8.16% (Fig. 11) of the total variance. This mode highlights the zonal dipole in the equatorial region, as detected in the second mode of the zonal currents. The negative signal covers the region of the cold tongue in the eastern equatorial Atlantic (Caniaux *et al.*, 2011), which is controlled by BF. In contrast, on the western of the TA, the positive signal covers the warm pool region, and to the north a positive signal is associated with NBC retroflection feeding the NECC.

The third mode (EOF3) represents 5.60%, (Fig. 12) of the total variance. The spatial pattern in the western TA shows high variability, with alternating signals of positive and negative values, however it is not a well-defined pattern. In the east TA there are well-defined structures of alternating signals of negative and positive anomalies, between 5ºS at 5ºN. (Fig. 12).
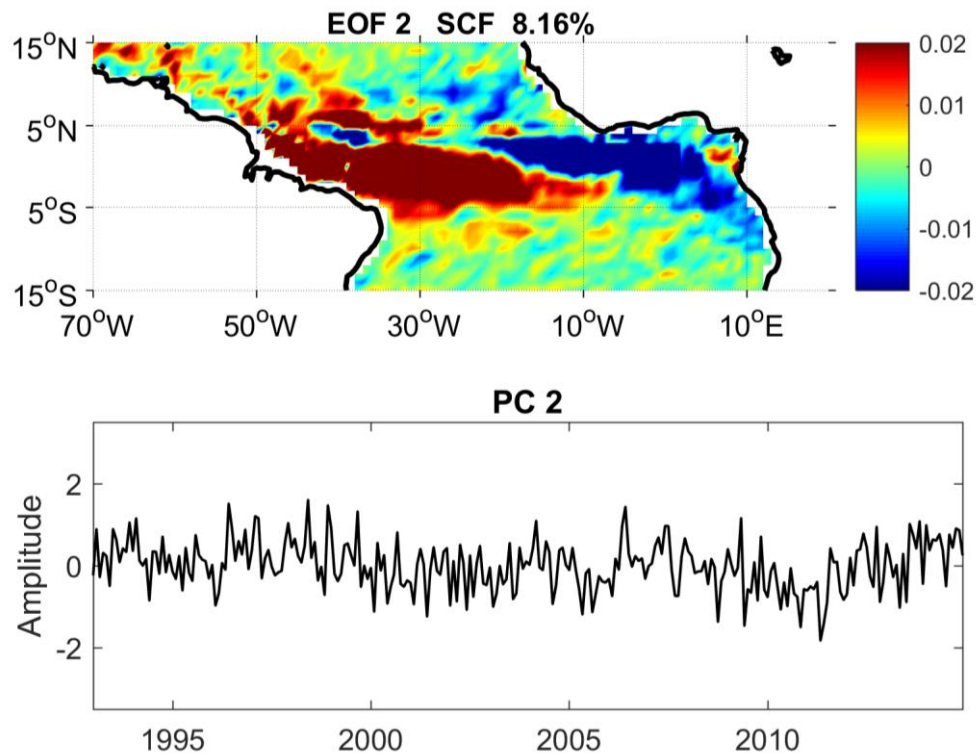
Tropical Oceanography, Recife, v. 46, n. 2, p. 1-24, 2018.

13

Figure 11. Second EOF mode of 22 years of the surface current speed, the Squared Covariance Fraction (SCF) in percentage, and the second Principal Component (PC2).
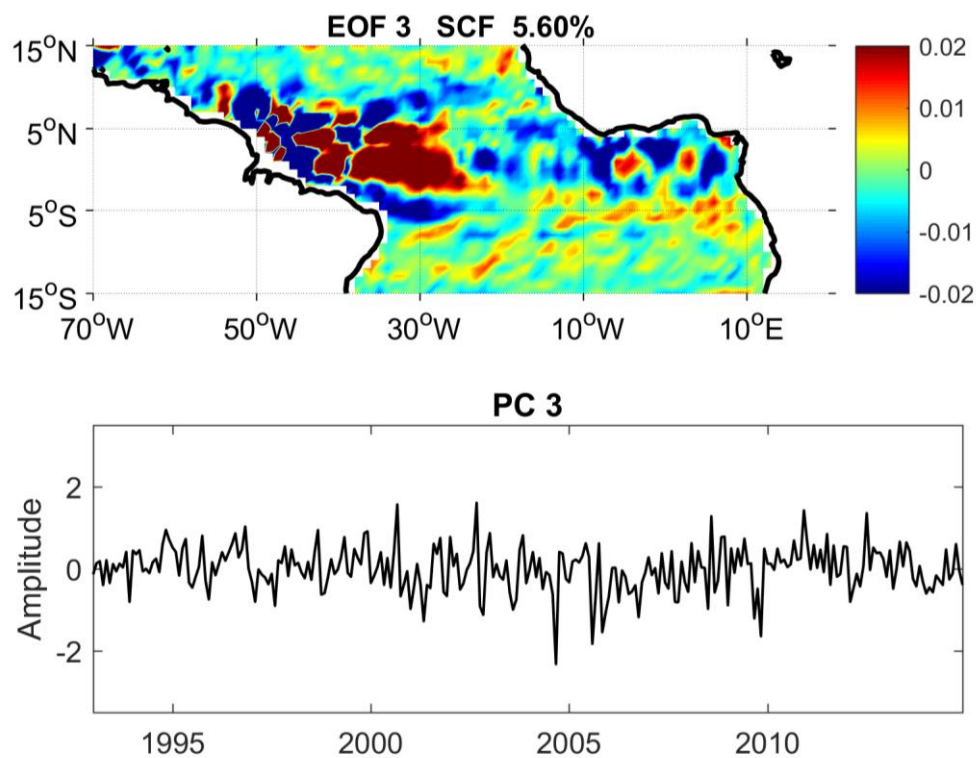

Figure 12. Third EOF mode of 22 years of the surface current speed, the Squared Covariance Fraction (SCF) in percentage, and the second Principal Component (PC3).

Tropical Oceanography, Recife, v. 46, n. 2, p. 1-24, 2018.

14

WAVELET ANALYSIS OF THE SURFACE CURRENT VELOCITIES

Since the PCs showed similar pattern with high frequency oscillations, wavelet analyses were performed for the PCs of each mode of surface currents (Fig. 13). The PC1 wavelet analyses showed the stronger variance mainly between 2004 and 2005 with about 6-months periodicity. The negative phase of the Atlantic Niño present in 2004-2005 could explain the strong variance in the surface current velocities in these years, as identified in the PC1 of the zonal components. The PC2 showed a peak for 36-month period between 2004 and 2005. The PC3 showed three dominant periodicities of strong variance, the first was between 1996 and 1997 for 16-month period, the second was during the 2004 and 2005 with 16-month periodicity, and the third for the 24-month period between 2010 and 2011.
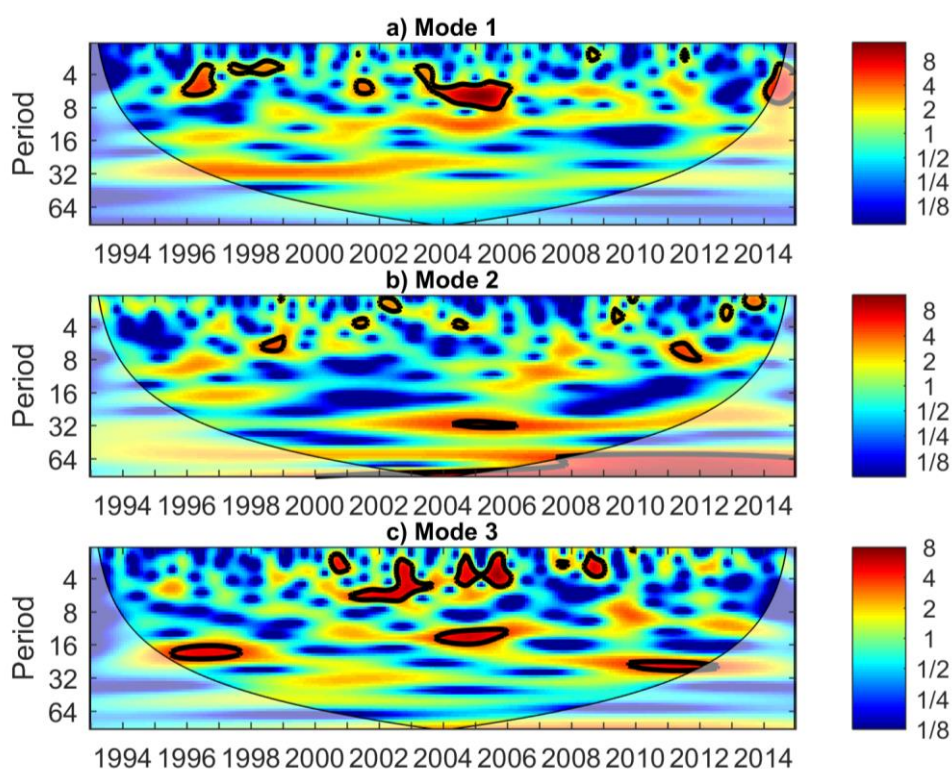

Figure 13. The wavelet transform of the Principal Components (PC1, PC2 and PC3) from the EOF1, EOF2 and EOF3 respectively of the surface current speed along the Tropical Atlantic.

DISCUSSION

The EOF analysis was applied to 22 years of current speed, zonal and meridional components, which allows identifying the main space-time variability in the Tropical Atlantic.

The first mode of the meridional component (18.77% of the total variance) identified structures of positive and negative cores (Fig. 2), mainly in the Western Tropical North Atlantic (WTNA). These structures indicate the high variability of this region, associated to NBC

retroflection and rings detachments, as well its westward propagations along the Guyana coast (Didden and Schott, 1993; Wilson *et al.*, 2002).

The EOF2 of the meridional component (11.98%) showed a similar pattern to the EOF1 (Fig. 2), with high dynamics in the WTNA, however expanding and weakening towards the eastern Atlantic. The successive modes of the meridional component show similar structures (EOFs 1, 2, 3, 4 and 5) with negative and positive cores in the WTNA. The main difference between these signals in the WTNA, in the modes 1 to 5, is the zonal shift of these structures and their relative intensities, corroborating with the high dynamics identified in this region, as the NBC retroflection (east to 7ºN and 52º W) and formations of anticyclonic rings. Furthermore, the NBC rings may be responsible for more than half of the interhemispheric transport of mass and heat associated with the meridional overturning circulation's upper limb (Garzoli *et al.*, 2003).

In the eastern TA, different patterns were identified. In the EOFs 1 to 5, alternating positive and negative signals were detected, but in the most cases these structures are not well identified. Except in the EOF2 and EOF5, where visible structures of opposite signals are stronger and evident. In the EOF5 these structures are strong, well defined and they propagate across the Atlantic basin, interacting with the WTNA structures. Despite these patterns have been detected with monthly data, they present structures like TIWs. According Legeckis (1977) and Legeckis *et al.* (1983), the TIWs have a wavelength of about 1000 km and a period of 30 days. Also, Evans *et al.* (2009) have identified these structures using monthly SST and chlorophyll data. Therefore, these structures found in EOFs 1 to 5 present the same pattern found in Decco *et al.* (2016). The TIWs propagates westward of the equatorial thermal (Decco *et al.*, 2016), driving energy as heat from tropical regions to other regions of the world (Cox, 1980; Weisberg and Horigan, 1981). Sea level fluctuations associated with TIWs are strong in the regions between 2° N to 5° N and 2° S to 5° S, and at west of 10° W (Han *et al.*, 2008; Schuckmann *et al.*, 2008).

The EOF of the first three zonal components account for more than 80% of the total variance. The first mode of the zonal component (50.73%) identified a large structure of negative signal at approximately 5°S – 5ºN (Fig. 6). This large and negative signal is associated with the central branch of the South Equatorial Current (cSEC) and part of this negative pattern also covers the area of the northern South Equatorial Current (nSEC), which is about 2ºN and 3°N (Urbano *et al*., 2008). This negative signal also flows along the north of Brazilian coast, representing the NBC. Further north, between 5ºN-7°N, a positive signal indicates an eastward flow, characterizing the NECC position (Fig. 6). The NECC flows generally eastward between about 3º–10ºN (Hormann *et al.*, 2012), bounded at north by the westward North Equatorial Current (NEC) and at the south by the westward nSEC.

Tropical Oceanography, Recife, v. 46, n. 2, p. 1-24, 2018.

16

The second mode of zonal component (8.23%) (Fig. 7) shows a zonal dipole with a positive signal in the west and a negative in the eastern TA. The negative signal in the eastern TA covers the area of the cold tongue, near African coast. The formation of the Atlantic cold tongue (ACT) is the dominant seasonal SST signal in the eastern equatorial Atlantic (Caniaux *et al.*, 2011).

The ACT reaches its peak in July–August (Okomura and Xie, 2004), from September onward, the upwelling is reduced through weakening of the southerly cross–equatorial winds (Deppenmeier *et al.*, 2016). De Almeida and Nobre (2012) have analysed the covariability of the trade winds over the western part of the basin, with SST and heat content in eastern TA. These mechanisms compose the Bjerknes Feedback (BF), which is responsible for the ACT mode. The ACT has a positive feedback phase peaking during boreal summer, when the BF is stronger. The negative signal identified in the eastern TA (Fig. 7) evidences that, it could be a response to the first BF component, once that the westward zonal currents are forced by the intensification of the southeasterly winds. Also, the strongest variance in the PC2 of the zonal component coincides with a negative phase of the Atlantic Niño in 2004-2005. Besides that, the positive signal in the west (Fig. 7) shows an inverse signal, associated to the warm pool region.

The third mode (5.67%) showed a negative axis crossing the Atlantic basin, similar to that identified in the EOF1. In this case, this signal is narrower and confined between 0 and 5° N, which could be related to a meridional shift of the cSEC. To the west, this negative signal follows the north Brazilian coast, as the NBC. This signal is bounded at north and south by two positive axes, indicating an eastward flow. The south positive pattern is limited at 5° S and 0° and could indicate a weakening of the cSEC. At north, the positive signal is established at 5°N - 7°N and coincides with the NECC position.

The first three modes of surface current velocities explain about 43% of the variance. The first mode of current speed (~ 30.0%) shows a dominant negative signal covering a broad area between 5°S-5°N and crossing the Atlantic basin. This signal is related with the cCSE, which flows towards the west. In contrast, a positive and weak signal at 7° N exists but it is not well defined as a pattern of current.

The second mode of current speed (8.16%) shows a zonal dipole (Fig. 11). In the western TA a positive signal exists covering the area of the Warm Pool. In the eastern TA, a negative pattern is predominant in the cold tongue. This pattern is similar to the EOF2 of the zonal component, which is about 28% of the variance. This pattern reinforces about the importance of this zonal dipole, also representing a mode controlled by the Bjerknes Feedback.

The third mode of the current velocities (EOF3 5.60%) shows a positive signal in the western TA (Fig. 12). Besides that, the third mode represent a small part of the variance, the pattern identified in the eastern TA shows a well-defined intermittent structure of alternating

Tropical Oceanography, Recife, v. 46, n. 2, p. 1-24, 2018.

17

positive and negative signal. This pattern is similar to the EOF2 of the meridional component (~12%), that could be associated to the Tropical Instability Waves.

SUMMARY AND CONCLUSIONS

In this study, we used 22 years dataset of monthly zonal and meridional surface currents to analyse their main modes of surface circulation variability in the Tropical Atlantic.

The EOFs of the meridional component identified variance, represented by the three first three modes, suggest high variability associated to North Brazil Current (NBC) retroflection and rings detachments in the WTNA and the TIWs in the eastern TA. Detect the main modes of variance in this region is important, once the NBC variability and rings are important for the ocean-atmosphere exchange climate implications, since they contribute for more than half inter-hemispheric transference of heat and mass (Garzoli *et al.*, 2003), propagating westward along the Guyana coast (Didden and Schott, 1993; Wilson *et al.*, 2002). Besides, the three main modes also indicated patterns associated to the propagation of TIWs westward along the equator (Decco *et al.*, 2016), which is an important conduct of heat from tropical regions to other parts of the planet (Cox, 1980; Weisberg and Horigan, 1981).

The first mode of zonal component identifies negative crossing basin signal representing the predominant transport westward by the zonal currents. This negative signal covers the Central South Equatorial Current (cSEC), part of area of the Northern South Equatorial Current (nSEC), and along the WTNA where the NBC flows. Further north, a positive signal showed an eastward flow, characterizing the North Equatorial Countercurrent (NECC) position. The zonal EOF2 (~8% of variance) detected a zonal dipole with a positive signal in the western, and a negative in the ACT region. Quantify the contribution of this pattern to the TA variability is important, once the ACT is associated with the highest concentrations of Chl-a in the TA, which occurs from $20°$ to $10°W$ and between $1°S$ and the equator, with a main seasonal peak in June–August (Jouanno *et al.*, 2011).The EOF3 is similar to that identified in the EOF1, however in this case, this signal is confined between $0°$ and $5°N$, which could be related to a meridional northward shift of the cSEC. There are two positive signals, the south signal could indicate a weakening of the cSEC, and the north coincides with the NECC position.

In the surface current speed analysis, we can infer the dominant role of the zonal component in the TA. EOF1 (~30%) showed a dominant negative signal covering a large area crossing the Atlantic basin, related to the cCSE in which flows westward. The EOF2 (8.16%) showed the importance of the zonal dipole, similar in the spatial pattern and variance to the zonal EOF2 (8.23%) of the zonal component. This pattern in the western of TA covers the area of the Warm Pool and the cold tongue area at the eastern of TA. Thus, the large-scale surface circulation in the TA is characterized by strong zonal variability and this upper-ocean zonal

Tropical Oceanography, Recife, v. 46, n. 2, p. 1-24, 2018.

18

current system is very important for the interhemispheric and west-to-east exchange of heat, salt and nutrients (Brandt *et al.*, 2008, Foltz *et al.*, 2003, Kirchner *et al.*, 2009).

The results of this work contribute to the understanding of the surface currents dynamics, zonal and meridional transport variability, and ocean-atmosphere interaction processes. As well as studies of air-sea CO_2 exchanges, nutrients, heat and mass distribution in the TA, besides that, this study has also the potential base line for further investigations associated to climatic signals.

ACKNOWLEDGEMENTS

REFERENCES

Arnault, S. and Kestenare, E. (2004), Tropical Atlantic surface current variability from10 years of TOPEX/Poséïdon altimetry, *Geophysical Research Letters*, Vol. 31, L03308 (pp. 1-4), doi:10.1029/2003GL019210.

Bakun, A. (1978), Guinea Current upwelling, *Nature*, Vol. 271, pp. 147–150, doi: 10.1038/271147a0.

Brandt, P., Hormann, V., Bourlès, B., Fischer, J., Schott, F.A., Stramma, L. and Dengler, M. (2008), Oxygen tongues and zonal currents in the equatorial Atlantic, *Journal of Geophysical Research*, Vol. 113, C04012 (pp. 1-15), doi:10.1029/2007JC004435.

Bonjean, F. and Lagerloef, G.S. (2002), Diagnostic Model and Analysis of the Surface Currents in the Tropical Pacific Ocean, *Journal of Physical Oceanography*, Vol. 32, pp. 2938–2954, doi: 10.1175/1520-0485(2002)032<2938:DMAAOT>2.0.CO;2.

Bourlès, B., Gouriou, Y. and Chuchla, R. (1999), On the circulation in the upper layer of the western equatorial Atlantic, *Journal of Geophysical Research*, Vol. 104, issue C9, pp. 21151–21170, doi: 10.1029/1999JC900058.

Bretherton, C., Smith, C. and Wallace, J. (1992), An Intercomparison of methods for finding coupled patterns in climate data, *Journal of Climate,* Vol. 5, pp. 541–560, doi:10.1175/1520-0442(1992)005%3C0541:AIOMFF%3E2.0.CO;2.

Caniaux, G., Giordani, H., Redelsperger, J.L., Guichard, F., Key, E. and Wade, M. (2011), Coupling between the Atlantic cold tongue and the West African monsoon in boreal spring

Tropical Oceanography, Recife, v. 46, n. 2, p. 1-24, 2018.

19

and summer, *Journal of Geophysical Research*, Vol. 116, C04003 (pp. 1-17), doi: 10.1029/2010JC006570.

Chang, P., Zhang, R., Hzeleger, W., Wen, C., Wan, X., Link, J., Haarsma, R.J., Breugem, W.P. and Seidel, H. (2008), Oceanic link between abrupt changes in the North Atlantic Ocean and the African monsoon, *Nature Geoscience*, Vol. 1, pp. 444–448, doi: 10.1038/ngeo218.

Coles, V.J., Brooks, M.T., Hopkins, J., Stukel, M.R., Yager, P.L., and Hood, R.R. (2013), The pathways and properties of the Amazon River plume in the tropical North Atlantic Ocean, *Journal of Geophysical Research,* Vol. 118, pp. 6894–6913, doi: 10.1002/2013JC008981.

Cox, M.D. (1980), Generation and Propagation of 30-Day Waves in a Numerical Model of the Pacific, *Journal of Physical Oceanography*, Vol. 10, pp. 1168–1186, doi:10.1175/1520-0485(1980)010<1168:GAPODW>2.0.CO;2.

De Almeida, R.A.F. and Nobre, P. (2012), On the Atlantic cold tongue mode and the role of the Pacific ENSO, *Ocean Science*, Discussion, Vol. 9, pp. 163-185, doi: 10.5194/osd-9-163-2012.

Decco, H.T. de, Rebelo, A., Junior, T., Pezzi, L.P. and Landau, L. (2016), Revisiting tropical instability wave variability in the Atlantic Ocean using SODA reanalysis, *Ocean Dynamics,* Vol. 68, pp. 327–345, doi:10.1007/s10236-017-1128-2.

Deppenmeier, A.L., Haarsma, R.J. and Hazeleger, W. (2016), The Bjerknes feedback in the tropical Atlantic in CMIP5 models, *Climate Dynamics*, Vol. 47, pp. 2691-2707, doi:10.1007/s00382-016-2992-z.

Didden, N. and Schott, F. (1993), Eddies in the North Brazil Current retroflection region observed by Geosat altimetry, *Journal of Geophysical Research*, Vol. 98, issue C11, pp. 20121–20131, doi: 10.1029/93JC01184.

Dohan, K., and Maximenko, N. (2010), Monitoring ocean currents with satellite sensors, *Oceanography*, Vol. 23, pp. 94–103, doi: 10.5670/oceanog.2010.08.

Dohan, K. (2017), Ocean surface currents from satellite data, *Journal of Geophysical Research,* Vol. 122, pp. 2647–2651, doi:10.1002/2017JC012961.

Doi, T., Tozuka, T., Sasaki, H., Masumoto, Y. and Yamagata, T. (2007), Seasonal and interannual variations of oceanic conditions in the Angola Dome, *Journal of Physical Oceanography,* Vol. 37, pp. 2698–2713, doi: 10.1175/2007JPO3552.1.

Evans, W.W., Strutton, P.G. and Chavez, F.P. (2009), Impact of tropical instability waveson nutrient and chlorophyll distributions in the equatorial Pacific, *Deep-Sea Research I*, Vol. 56, pp. 178–188.

Fratantoni, D.M. and Glickson, D.A. (2002), North Brazil Current Ring Generation and Evolution Observed with SeaWiFS*, *Journal of Physical Oceanography*, Vol. 32, pp. 1058–1074, doi: 10.1175/1520-0485(2002)032<1058:NBCRGA>2.0.CO;2.

Flagg, C.N., Gordon, R.L. and McDowell, S. (1986), Hydrographic and Current Observations on the Continental Slope and Shelf of the Western Equatorial Atlantic, *Journal of Physical*

Tropical Oceanography, Recife, v. 46, n. 2, p. 1-24, 2018.

20

Oceanography, Vol. 16, pp. 1412–1429, doi: 10.1175/1520-0485(1986)016<1412:HACOOT>2.0.CO;2.

Foltz, G.R., Grodsky, S.A., Carton, J.A. and McPhaden, M.J. (2003), Seasonal mixed layer heat budget of the Tropical Atlantic Ocean, *Journal of Geophysical Research*, Vol. 108, issue C5, pp. 3146-3159, doi: 10.1029/ 2002JC001584.

Fonseca, C.A., Goni, G.J., Johns, W.E. and Campos, E.J.D. (2004), Investigation of the North Brazil Current retroflection and North Equatorial Countercurrent variability, *Geophysical Research Letters.*, Vol. 31, L21304, doi: 10.1029/2004GL020054.

Ganachaud, A. and Wunsch, C. (2000), Improved estimates of global ocean circulation, heat transport and mixing from hydrographic data, *Nature*, Vol. 408, pp. 453–457, doi:10.1038/35044048.

Garzoli, S.L., Ffield, A., Johns, W.E. and Yao, Q. (2004), North Brazil Current retroflection and transports, *Journal of Geophysical Research*, Vol. 109, C01013, doi: 10.1029/2003JC001775.

Garzoli, S.L., Ffield, A. and Yao, Q. (2003), North Brazil Current rings and the variability in the latitude of the retroflection, in Goni, G.J. and Malanotte-Rizzoli, P. (eds.), *Interhemispheric Water Exchange in the Atlantic Ocean*, Elsevier Oceanography Series, ISBN 0444512675, Vol. 68, pp. 357–373.

Geyer, W.R., Beardsley, R.C., Lentz, S.J., Candela, J., Limeburner, R., Johns, W.E., Castro, B.M. and Soares, I.D. (1996), Physical oceanography of the Amazon shelf, *Continental Shelf Research*, Vol. 16, pp. 575-616, doi: 10.1016/0278-4343(95)00051-8.

Gordon, A.L. (1986), Interocean exchange of thermocline water, *Journal of Geophysical Research*, Vol. 91, pp. 5037–5046, doi:10.1029/JC091iC04p05037.

Han, W., Webster, P.J., Lin, J.-L., Liu, W.T., Fu, R., Yuan, D. and Hu, A. (2008), Dynamics of intraseasonal sea level and thermocline variabilityin the equatorial Atlantic during 2002-03, *Journal of Physical Oceanography*, Vol. 38, pp. 945–967. doi:10.1175/2008JPO3854.1.

Hardman-Mountford, N.J., Richardson, A.J., Agenbag, J.J., Hagen, E., Nykjaer, L., Shillington, F.A. and Villacastin, C. (2003), Ocean climate of the South East Atlantic observed from satellite data and wind models, *Progress in Oceanography*, Vol. 59, pp. 181–221, doi:10.1016/j.pocean.2003.10.001.

Hormann, V. and Brandt, P. (2009), Upper equatorial Atlantic variability during 2002 and 2005 associated with equatorial Kelvin waves, *Journal of Geophysical Research*, Vol. 114, C03007, doi: 10.1029/2008JC005101.

Hormann, V., Lumpkin, R. and Foltz, G.R. (2012), Interannual North Equatorial Countercurrent variability and its relation to tropical Atlantic climate modes, *Journal of Geophysical Research*, Vol. 117, C04035, doi: 10.1029/2011JC007697.

Jochum, M. and Malanotte-Rizzoli, P. (2003), On the generation of North Brazil Current rings, *Journal of Marine Research,* Vol. 61, pp. 147–173, doi: 10.1357/002224003322005050.

Tropical Oceanography, Recife, v. 46, n. 2, p. 1-24, 2018.

21

Johnson, E.S., Bonjean, F., Lagerloef, G.S., Gunn, J.T. and Mitchum, G.T. (2007), Validation and Error Analysis of OSCAR Sea Surface Currents, *Journal of Atmospheric and Oceanic Technology*, Vol. 24, pp. 688–701, doi: 10.1175/JTECH1971.1.

Johns, W.E., Lee, T.N., Schott, F.A., Zantopp, R.J. and Evans, R.H. (1990), The North Brazil Current retroflection: Seasonal structure and eddy variability, *Journal of Geophysical Research*, Vol. 95, issue C12, pp. 22103–22120, doi: 10.1029/JC095iC12p22103.

Johns, W.E., Lee, T.N., Beardsley, R.C., Candela, J., Limeburner, R. and Castro, B. (1998), Annual cycle and variability of the North Brazil Current, *Journal of Physical Oceanography,* Vol. 28, pp. 103–128, doi: 10.1175/1520-0485(1998)028<0103:ACAVOT>2.0.CO;2.

Jouanno, J., Marin, F., du Penhoat, Y., Sheinbaum, J. and Molines, J.M. (2011), Seasonal heat balance in the upper 100 m of the equatorial Atlantic Ocean, *Journal of Geophysical Research*, Vol. 116, C09003, doi: 10.1029/2010JC006912.

Longhurst, A.R. (1962), A review of the oceanography of the Gulf of Guinea, *Bulletin de L'Institute Français d'Afrique Noire*, Vol. 24, pp. 633–663.

Legeckis, R. (1977), Long waves in the eastern equatorial Pacific Ocean: A view from a geostationary satellite, *Science*, Vol. 197, pp. 1179-1181.

Legeckis, R., Pichel, W. and Nesterczuk, G. (1983), Equatorial long waves in geostationary satellite observations and in a multichannel sea surface temperature analysis, *Bulletin of the American Meteorological Society*, Vol. 64, pp. 133-139.

Kirchner, K., Rhein, M., H€uttl-Kabus, S. and Böning, C.W. (2009), On the spreading of South Atlantic Water into the Northern Hemisphere, *Journal of Geophysical Research*, Vol. 114, C05019, doi:10.1029/2008JC005165.

Mazeika, P.A. (1967), Thermal domes in the eastern tropical Atlantic Ocean, *Limnology and Oceanography*, Vol. 12, pp. 537–539, doi: 10.4319/lo.1967.12.3.0537.

Mittelstaedt, E. (1983), The upwelling area off Northwest Africa - a description of phenomena related to coastal upwelling, *Progress in Oceanography*, Vol. 12, pp. 307-331, doi: 10.1016/0079-6611(83)90012-5.

Muller-Karger, F.E., Varela, R., Thunell, R., Luerssen, R., Hu, C. and Walsh, J.J. (2005), The importance of continental margins in the global carbon cycle, *Geophysical Research Letters*., Vol. 32, L01602, doi: 10.1029/2004GL021346.

Oh, J. and Suh, K. (2018), Real-time forecasting of wave heights using EOF – wavelet – neural network hybrid model, *Ocean Engineering*, Vol. 150, pp. 48–59, doi:10.1016/j.oceaneng.2017.12.044.

Okumura, Y. and Xie, S. (2004), Interaction of the Atlantic Equatorial Cold Tongue and the African Monsoon, *Journal of Climate*., Vol. 17, pp. 3589–3602, doi:10.1175/1520-0442(2004)017.<3589:IOTAEC>2.0.CO;2

Peter, A.-C., Le He′naff, M., Du Penhoat, Y., Menkes, C.E., Marin, F., Vialard, J., Caniaux, G. and Lazar, A. (2006), A model study of the seasonal mixed layer heat budget in the equatorial Atlantic, *Journal of Geophysical Research*, Vol. 111, C06014, doi:10.1029/2005JC003157.

Tropical Oceanography, Recife, v. 46, n. 2, p. 1-24, 2018.

22

Peterson, R.G. and Stramma, L. (1991), Upper-level circulation in the South Atlantic Ocean, *Progress in Oceanography*, Vol. 26, pp. 1-73, doi: 10.1016/0079-6611(91)90006-8.

Richardson, P.L., Hufford, G.E., Limeburner, R. and Brown, W.S. (1994), North Brazil Current retroflection eddies, *Journal of Geophysical Research*, Vol. 99, issue C3, pp. 5081–5093, doi: 10.1029/93JC03486.

Richardson, P.L. and Reverdin, G. (1987), Seasonal cycle of velocity in the Atlantic North Equatorial Countercurrent as measured by surface drifters, current meters, and ship drifts, *Journal of Geophysical Research,* Vol. 92, pp. 3691–3708, doi: 10.1029/JC092iC04p03691.

Richardson, P.L. and Walsh, D. (1986), Mapping climatological seasonal variations of surface currents in the tropical Atlantic using ship drifts, *Journal of Geophysical Research*, Vol. 91, issue C9, pp. 10537–10550, doi: 10.1029/JC091iC09p10537.

Rodrigues, R.R., Rothstein, L.M. and Wimbush, M. (2007), Seasonal Variability of the South Equatorial Current Bifurcation in the Atlantic Ocean: A Numerical Study, *Journal of Physical Oceanography*, Vol. 37, pp. 16–30, doi: 10.1175/JPO2983.1.

Schmitz Jr., W.J (1995), On the interbasin-scale thermohaline circulation, *Reviews of Geophysics*, Vol. 33, pp. 151–173, doi:10.1029/95RG00879.

Servain, J., Picaut, J. and Merle, J. (1982), Evidence of remote forcing in the equatorial Atlantic ocean, *Journal of Physical Oceanography,* Vol. 12, pp.457–463, doi:10.1175/1520-0485(1982)012<0457:EORFIT>2.0.CO;2.

Silveira, I.C. A. da, Miranda, L.B. de and Brown, W.S. (1994), On the origins of the North Brazil Current, *Journal of Geophysical Research*, Vol. 99, issue C11, pp. 22501–22512, doi: 10.1029/94JC01776.

Schouten, M.W., Matano, R.P. and Strub, T.P. (2005), A description of the seasonal cycle of the equatorial Atlantic from altimeter data, *Deep-Sea Research I*, Vol. 52, pp. 477 – 493, doi: 10.1016/j.dsr.2004.10.007.

Schott, F.A., Dengler, M., Zantopp, R., Stramma, L., Fischer, J. and Brandt, P. (2005), The Shallow and Deep Western Boundary Circulation of the South Atlantic at 5°–11°S, *Journal of Physical Oceanography*, Vol. 35, pp. 2031–2053, doi: 10.1175/JPO2813.1.

Stramma, L. and England, M. (1999), On the water masses and mean circulation of the South Atlantic Ocean, *Journal of Geophysical Research*, Vol. 104, issue C9, pp. 20863–20883, doi: 10.1029/1999JC900139.

Stramma, L. and Schott, F. (1999), The mean flow field of the tropical Atlantic Ocean, *Deep-Sea Research II*, Vol. 46, pp. 279–303, doi: 10.1016/S0967-0645(98)00109-X.

Stramma, L., Rhein, M., Brandt, P., Dengler, M., Böning, C. and Walter, M. (2005), Upper ocean circulation in the western tropical Atlantic in boreal fall 2000, *Deep-Sea Research I*, Vol. 52, pp. 221–240. doi:10.1016/j.dsr.2004.07.021.

Sudre, J. and Morrow, R.A. (2008), Global surface currents: A high-resolution product for investigating ocean dynamics, *Ocean Dynamics*, Vol. 58, pp. 101–118, doi:10.1007/s10236-008-0134-9.

Urbano, D.F., De Almeida, R.A.F. and Nobre, P. (2008), Equatorial Undercurrent and North Equatorial Countercurrent at 38ᵒW: A new perspective from direct velocity data, *Journal of Geophysical Research*, Vol. 113, C04041, doi: 10.1029/2007JC004215.

Veleda, D., Araujo, M., Zantopp, R. and Montagne, R. (2012), Intraseasonal variability of the North Brazil Undercurrent forced by remote winds, *Journal of Geophysical Research*, Vol. 117, C11024, doi: 10.1029/2012JC008392.

von Schuckmann, K., Brandt, P. and Eden, C. (2008), Generation of tropical instability waves in the Atlantic Ocean, *Journal of Geophysical Research*, Vol. 113, C08034, doi: 10.1029/2007JC004712.

Wallace, J., Smith, C. and Bretherton, C. (1992), Singular value decomposition of Wintertime Sea surface temperature and 500-mb height anomalies, *Journal of Climate,* Vol. 5, pp. 561–576, doi: 10.1175/1520-0442(1992)005%3C0561:SVDOWS%3E2.0.CO;2.

Weisberg, R.H. and Horigan, A.M. (1981), Low-frequency variability in the equatorial Atlantic, *Journal of Physical Oceanography,* Vol. 11, pp. 913–920, doi: 10.1175/1520-0485(1981)011<0913:LFVITE>2.0.CO;2.

Wilson W.D., Johns, W.E. and Garzoli, S.L. (2002), Velocity structure of North Brazil Current rings, *Geophysical Research Letters*, Vol. 29, issue 8, pp. 114-1–114-3, doi: 1029/2001GL013869.

Yamagata, T. and Iizuka, S. (1995), Simulation of the Tropical Thermal Domes in the Atlantic: A Seasonal Cycle, *Journal of Physical Oceanography*, Vol. 25, pp. 2129–2140, doi:10.1175/1520-0485(1995)025%3c2129:SOTTTD%3e2.0.CO;2.

Yoder, J.A. and Kennelly, M.A. (2003), Seasonal and ENSO variability in global ocean phytoplankton chlorophyll derived from 4 years of SeaWiFS measurements, *Global Biogeochemichal Cycles*, Vol. 17, pp. 1112, doi: 10.1029/2002GB001942, 4.

Tropical Oceanography, Recife, v. 46, n. 2, p. 1-24, 2018.

24